31st EPS Conference on Plasma Phys. London, 28 June - 2 July 2004 ECA Vol.**28G**, P-1.210 (2004)

Density, Electron Temperature and Electric Potential Fluctuations and Induced Radial Transport in the Boundary of the Wendelstein 7-AS Stellarator from a Poloidal Array of Langmuir Probes

M. Schubert, M. Endler, and W7-AS Team

Max-Planck-Institut für Plasmaphysik, EURATOM Association, Garching/Greifswald, Germany

1 Diagnostic System and Data Analysis

A poloidal array of 15 graphite tips, each $1\,mm$ in diameter with a spacing of $2\,mm$ in between them, was used in the Wendelstein 7-AS (W7-AS) stellarator scrape-off layer (SOL) to investigate fluctuations of plasma density n, electron temperature T_e and plasma potential U_pl. To this end, the tip voltage is sinusoidally swept with a frequency of 1.4 MHz, and the resulting currents on individual tips are recorded with fast analog-to-digital converters at a sampling rate of 50 MHz.

This method was applied before [1, 2] and, with a related approach, in [3], with an analysis of up to 3 tips. In the earlier work, the sweep frequency of several 100 kHz was found to be marginal, since the fluctuation amplitude is still significant in this frequency range. We have improved the electronics for amplifying the fast swept signals, which requires unusual high common mode rejection at voltages of up to 100 V. Additionally, we have for the first time extended the technique to a spatially resolving array of 15 Langmuir probe tips. This allows us to analyse the relative phase between fluctuating quantities and the contributions to the radial transport of the individual Fourier components in frequency and wave number space.

The probe array is mounted on a fast reciprocating drive, such that radial profiles of the measured quantities are obtained in single discharges. In order to calculate the fluctuating plasma quantities from the recorded probe characteristics, for each probe tip the parameters I_sat, U_fl and T_e of the theoretical current-voltage characteristic

$$I(U) = I_\mathrm{sat}\left(1 - \exp\left(\frac{e(U - U_\mathrm{fl})}{k_\mathrm{B} T_\mathrm{e}}\right)\right)$$

are numerically fitted to the recorded $I(U)$ values for each half period. We then use a one-dimensional model by Emmert [4] including both presheath and sheath potential drop to calculate n and U_pl from I_sat, U_fl and T_e. The more commonly used model, which just assumes sound velocity c_s at the sheath edge (Bohm criterion) results in

$$U_\mathrm{pl} \;=\; U_\mathrm{fl} \;+\; \frac{k_\mathrm{B}\, T_\mathrm{e}}{e} \cdot \ln\left((1 - \gamma_\mathrm{SE})\sqrt{\frac{m_\mathrm{i}}{2\pi m_\mathrm{e}}\,\frac{T_\mathrm{e}}{T_\mathrm{e} + T_\mathrm{i}}}\;\right)$$

and

$$I = A\,\frac{n}{2}\,\left(c_\mathrm{s} - \frac{\bar{c}_\mathrm{e}}{2}\,\exp\left(\frac{e(U-U_\mathrm{pl})}{k_\mathrm{B}T_\mathrm{e}}\right)\right).$$

This model yields similar results for the average values as the Emmert model. For the ion temperature we assume $T_i \equiv \bar{T}_e$ for lack of better knowledge.

In our nonlinear fit model for the $I(U)$ characteristics, the fit parameters can become covariant if the samples deviate from the ideal exponential curve. Reasons for a deviation can be either electronic noise or a change of plasma parameters during one sweep. The latter is relevant if frequency components of the fluctuationg quantities not much below the sweep frequency still contain significant power in the probe tip frame of reference, e.g. due to fast poloidal E×B rotation. This is the case when the probe approaches the separatrix and the shear layer. The covariance of two quantities will show up as non-

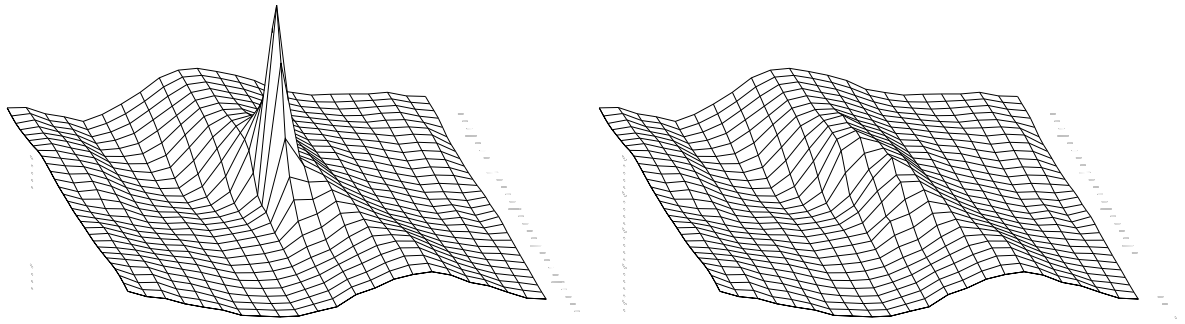

Figure 1: Two-dimensional interpolation of spatio-temporal cross correlation functions, here between $\tilde{U}_\mathrm{fl}$ and $\tilde{T}_\mathrm{e}$.

zero correlation around zero time and space lag when calculating the cross correlation function between these quantities (see figure 1, left). Before transforming the correlation function into Fourier space we therefore mask the central peak and replace the missing values by a two-dimensional surface interpolation (see figure 1, right). The problems due to covariant fitting parameters have been pointed out before [2], but a satisfactory workaround is possible only now, as we have sufficient spatial resolution.

2 Results

Poloidal-temporal auto correlation functions of the fluctuating quantities have already been presented in [5]. Here, we focus on the cross correlation functions, cross spectra and relative phases between the different fluctuating quantities. As an example, the cross correlation function between U_fl and T_e, the corresponding cross kf power spectrum and phase spectrum are shown in fig. 2. The poloidal velocity of the structures is caused mainly by the E×B velocity due to the radial electric field. As this is positive (directed radially outwards) in the SOL of W7-AS, the propagation of the main feature of the correlation function is in the direction of the ion diamagnetic drift. The Fourier representation can be compared with the output of numerical simulations, and the poloidal wavenumber is therefore shown in units $1/\rho_\mathrm{s}$. The natural scale of drift wave models ρ_s is the ion sound velocity over ion cyclotron frequency, and in our case $\rho_\mathrm{s} = 0.03\,\mathrm{cm}$.

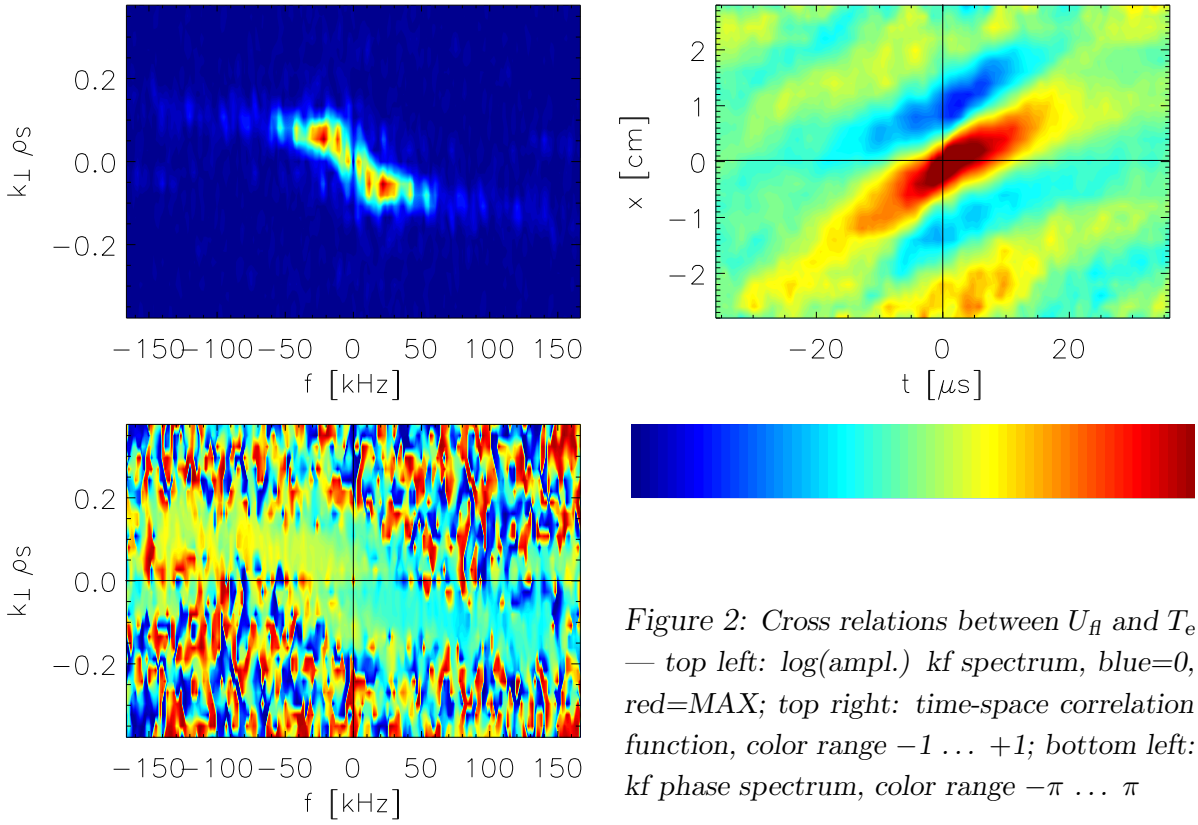

Figure 2: Cross relations between U_{fl} and T_e — top left: log(ampl.) kf spectrum, blue=0, red=MAX; top right: time-space correlation function, color range $-1 \ldots +1$; bottom left: kf phase spectrum, color range $-\pi \ldots \pi$

Note that the cross phase is comparatively constant where the Fourier components have significant power. We have therefore weighted the cross phase of one half plane of the kf spectrum with the cross power, and display radial profiles of the results for combinations between different quantities in fig. 3.

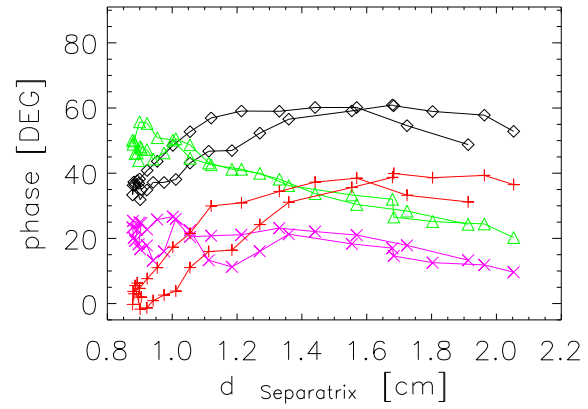

Figure 3: Radial profiles of power weighted cross phase between different quantities — black: between $\tilde{U}_{pl}$ and $\tilde{n}$; red: between $\tilde{T}_e$ and $\tilde{n}$; pink: between $\tilde{U}_{pl}$ and $\tilde{T}_e$; green: between $\tilde{U}_{fl}$ and $\tilde{T}_e$. Positive phases correspond to a time delay of the second quantity relative to the first one. Note that the phase of $\tilde{U}_{fl}$ can significantly deviate from the phase of $\tilde{U}_{pl}$.

3 Discussion and Conclusions

The power weighted cross phases between the fluctuating quantities display a remarkable radial variation: Whereas $\tilde{U}_{\mathrm{pl}}$ leads $\tilde{n}$ by 35–40° at the innermost probe position, this angle increases to 55–60° 1 cm farther outside the last closed magnetic surface (LCMS). At the same time, the lag between $\tilde{U}_{\mathrm{pl}}$ and $\tilde{T}_{\mathrm{e}}$ reduces from 20–25° to 10–15°, i. e., whereas $\tilde{n}$ and $\tilde{T}_{\mathrm{e}}$ are almost in phase close to the LCMS, the phase of $\tilde{T}_{\mathrm{e}}$ approaches the phase

of $\tilde{U}_{\mathrm{pl}}$ farther out in the SOL (see fig. 4).

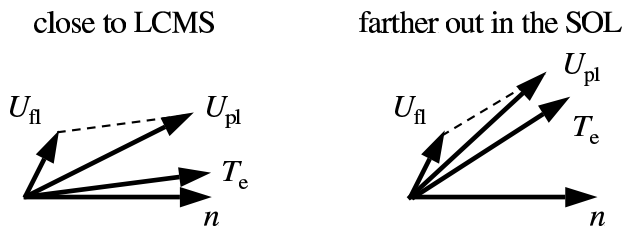

Figure 4: Comparison of the relative phase between different fluctuating quantities (represented as arrows in the complex plane) at different radial positions in the scrape-off layer (schematically, amplitudes not to scale).

Notwithstanding the fact that this result depends to a certain degree on the probe theory used in the calculation of $\tilde{n}$ and $\tilde{U}_{\mathrm{pl}}$ from the primary fit parameters $\tilde{I}_{\mathrm{sat}}$, $\tilde{T}_{\mathrm{e}}$ and $\tilde{U}_{\mathrm{fl}}$, such a trend would be expected if drift-Alfvén turbulence on closed flux surfaces still influences the fluctuations close to the LCMS, since in this case numerical computations predict small phase angles between $\tilde{n}$, $\tilde{T}_{\mathrm{e}}$ and $\tilde{U}_{\mathrm{pl}}$. In contrast, in the SOL, the flute-like target plate instability mechanism acts toward a phase angle of 90° between $\tilde{U}_{\mathrm{pl}}$ and $\tilde{n}$ [6]. In addition, the positive feedback between $\tilde{U}_{\mathrm{pl}}$ and fluctuating electron heat flux onto the target plates tends to reduce the phase angle between $\tilde{T}_{\mathrm{e}}$ and $\tilde{U}_{\mathrm{pl}}$, in particular in the presence of a low radial T_{e} gradient [7].

We have demonstrated that the simultaneous measurement of $\tilde{n}$, $\tilde{T}_{\mathrm{e}}$ and $\tilde{U}_{\mathrm{pl}}$ at multiple poloidal positions and the analysis of the radial variation of these fluctuations results in novel experimental information to be compared with numerical simulations of plasma turbulence in the transition region between closed and open magnetic surfaces. Since the relative phase between fluctuating quantities co-determines the induced turbulent transport, as a next step, the contributions of the different (k, f) components to the radial particle and electron heat transport will be analysed.

[1] R. Balbín et al., Rev. Sci. Instrum. **63** (1992) 4605; C. Hidalgo et al., Phys. Rev. Lett. **69** (1992) 1205; U. Pfeiffer et al., Contrib. Plasma Phys. **38** (1998) 134, Special issue, Proc. 3rd Int. Workshop on Electrical Probes in Magnetized Plasmas (1997), Berlin, Germany.

[2] L. Giannone et al., Phys. Plasmas **1** (1994) 3614.

[3] M. A. Meier et al., Rev. Sci. Instrum. **66** (1995) 437; M. A. Meier et al., Contrib. Plasma Phys. **38** (1998) 98, Special issue, Proc. 3rd Int. Workshop on Electrical Probes in Magnetized Plasmas (1997), Berlin, Germany.

[4] G. A. Emmert et al., Phys. Fluids **23** (1980) 803.

[5] M. Schubert et al., in 29th EPS Conf. (Montreux) (2002), paper P-3.218.

[6] A. V. Nedospasov, Soviet Journal of Plasma Physics **15** (1989) 659; X. Garbet et al., Nucl. Fusion **31** (1991) 967; M. Endler et al., Nucl. Fusion **35** (1995) 1307.

[7] M. Endler, PhD thesis, TU München, 1994, report IPP III/197.